9-27-1993

Gyroless line-of-sight stabilization for pointing and tracking systems

Marcelo C. Aigrain

Gyroless line-of-sight stabilization for pointing and tracking systems

Marcelo C. Algrain
University of Nebraska-Lincoln
Department of Electrical Engineering and
Center for Electro-Optics
209N Walter Scott Engineering Center
Lincoln, Nebraska 68588-0511
E-mail: marcelo@gaucho.unl.edu

Abstract. A new platform stabilization approach is described where miniature, low-cost, linear accelerometers are used (instead of gyroscopes) for line-of-sight (LOS) stabilization. This is accomplished by placing the accelerometers at strategic locations and combining their outputs so that angular motion is determined from linear acceleration measurements. The control system uses the sensed angular accelerations to generate movement commands for the gimbal servomotors in the stabilization platform. This counterrotates the imaging device to stabilize its LOS. The use of accelerometers allows the servo system to operate in an acceleration control mode, which is more desirable than position or velocity control modes, typical of gyro-based systems, since this increases stabilization bandwidth. Substituting gyros with accelerometers provides the additional benefits of lower sensor cost, weight, and power consumption, better temperature characteristics, more robustness, and higher shock resistance.

Subject terms: line of sight; stabilized platforms; linear accelerometers; gyroscopes.

Optical Engineering 33(4), 1255–1260 (April 1994).

1 Introduction

Sensing equipment such as electronic imaging devices, cameras, radar, navigation instruments, and the like is frequently carried by and operated in a moving vehicle, such as an airplane, that undergoes rotational motion about its center of rotation. In such an environment, the equipment is typically mounted on a movable platform that is stabilized with respect to vehicle movements. The purpose of a stabilized platform is to reject the angular disturbances so that the device modulation transfer function (MTF) is preserved at the system level. The stabilization may be about one, or more, of the vehicle axes. Particular applications involve the line-of-sight (LOS) stabilization of a camera or other imaging devices. In such cases, when the vehicle undergoes rotational motion about its axes, the LOS remains fixed with respect to an inertial reference frame. This is accomplished by sensing these angular disturbances and generating the necessary counterrotations. A significant cost driver in traditional stabilization systems is the gyroscope and its associated electronics. The cost of sensing angular disturbances using linear accelerometers is at least 7 to 10 times lower than that using traditional jewel-bearing gyros. Jewel-bearing gyro technology has remained static over many years. On the other hand, the size, weight, and cost of linear accelerometers are decreasing while their performance is improving. This trend is expected to continue. Therefore, the gyro versus accelerometer cost/performance ratios will increase, making the gyroless approach a desirable and cost-effective alternative. Accelerometers are also more robust and shock resistant than gyros and have a larger operational temperature range. This makes them more reliable in harsh environments.

2 Determining Angular Motion from Linear Measurements

Kinematically, the motion of a body can be explained geometrically by establishing the time-dependent relationships among its displacement, velocity, and acceleration. In so doing, it is frequently convenient to simultaneously use several frames of reference instead of a single inertial coordinate system. If one of these frames is designated as *fixed,* the choice is arbitrary; the others, not rigidly attached to it, are designated as *moving.* Considering the two moving particles P and Q in Fig. 1, the vectors $\mathbf{R}_P$ and $\mathbf{R}_Q$ give the position of the two particles at any given time with respect to the fixed frame XYZ attached to O. The vector $\mathbf{R}_{Q/P}$ gives the position of Q relative to the moving frame $X'Y'Z'$ attached to P. Then it can be concluded that the position of Q is obtained by summing the vector $\mathbf{R}_{Q/P}$ to the vector $\mathbf{R}_P$. The change rate of these vectors is obtained by differentiation, defining the velocities $\mathbf{V}_Q$, $\mathbf{V}_P$, and $\mathbf{V}_{Q/P}$. A second differentiation gives the acceleration vectors $\mathbf{A}_Q$, $\mathbf{A}_P$, and $\mathbf{A}_{Q/P}$. This procedure leads to the well-known expression[1] for the total acceleration of the particle Q (within the rigid body) with respect to an inertial coordinate frame attached to point O:

Paper 19063 received Jun. 21, 1993; accepted for publication Sep. 27, 1993.

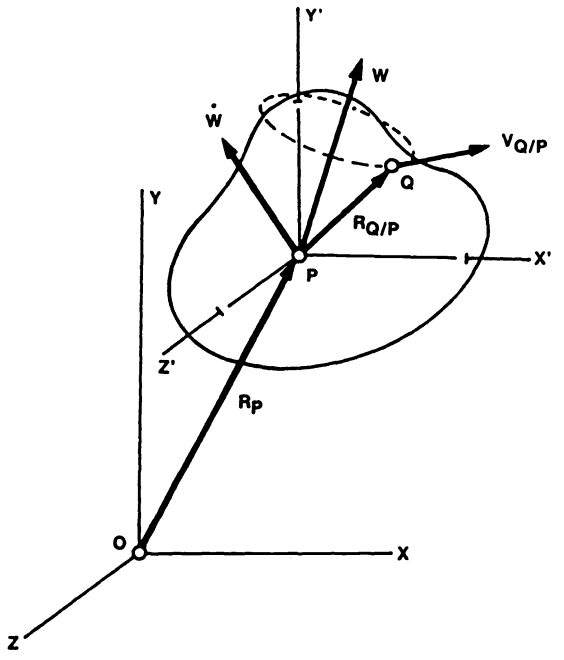

Fig. 1 Three-dimensional motion of rigid body.

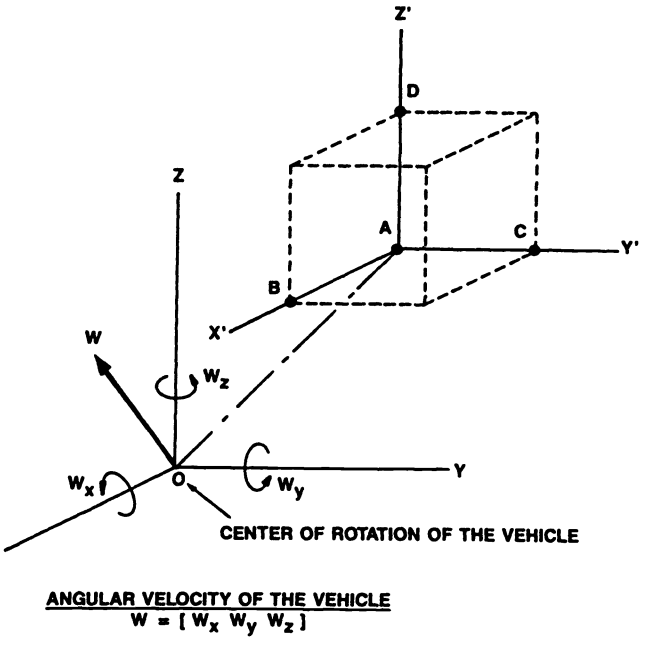

Fig. 2 Linear accelerometer arrangement of angular motion determination.

$$\mathbf{A}_Q = \mathbf{A}_P + \dot{\mathbf{W}} \times \mathbf{R}_{Q/P} + \mathbf{W} \times (\mathbf{W} \times \mathbf{R}_{Q/P}) \ , \tag{1}$$

where

$\mathbf{A}_P$ = acceleration of P with respect to O

$\dot{\mathbf{W}}$ = angular body acceleration

$\mathbf{W}$ = angular body velocity

$\mathbf{R}_{Q/P}$ = vector distance between P (start) and Q (end)

$\times$ = cross product operator.

Equation (1) shows that the most general motion of a rigid body is equivalent, at any given instant, to the sum of a translation (where all the body particles have the same acceleration as a reference particle P) and a rotation (where the particle P is assumed to be fixed). Therefore, total acceleration measurements provide indirect information of the body angular motion. Padgaonkar, Krieger, and King[2] and Schuler, Grammatikos, and Fegley[3] have shown how to separate the accelerations due to translation from those due to rotation through various accelerometer placement schemes. They obtain expressions for angular acceleration measurements based on linear accelerometer outputs. A past limitation of the technique has been its sensitivity to accelerometer cross-axis coupling effects.[4] However, newer accelerometer technology and manufacturing techniques have significantly reduced cross-axis sensitivity to less than a fraction of a percent in some devices; therefore, it is no longer a concern. Furthermore, recent developments in accelerometer technology have led to a new generation of solid-state devices that are smaller, lighter, more accurate, and less expensive than their predecessors.[5] These devices make measuring angular motion with linear accelerometers a cost-effective alternative to using angular sensors.

To illustrate this fact, consider the most general sensor arrangement shown in Fig. 2. Triaxial linear accelerometers are placed at points A, B, C, and D. Point O represents the center of vehicle rotation around which the angular velocity $\mathbf{W} = (W_X W_Y W_Z)^T$ is exerted. Making use of the expression for total acceleration, the linear accelerations at points A, B, C, and D are given by:

$$\mathbf{A}_A = \mathbf{A}_O + \dot{\mathbf{W}} \times \mathbf{R}_{A/O} + \mathbf{W} \times (\mathbf{W} \times \mathbf{R}_{A/O}) \ ,$$

$$\mathbf{A}_B = \mathbf{A}_A + \dot{\mathbf{W}} \times \mathbf{R}_{B/A} + \mathbf{W} \times (\mathbf{W} \times \mathbf{R}_{B/A}) \ ,$$

$$\mathbf{A}_C = \mathbf{A}_A + \dot{\mathbf{W}} \times \mathbf{R}_{C/A} + \mathbf{W} \times (\mathbf{W} \times \mathbf{R}_{C/A}) \ ,$$

$$\mathbf{A}_D = \mathbf{A}_A + \dot{\mathbf{W}} \times \mathbf{R}_{D/A} + \mathbf{W} \times (\mathbf{W} \times \mathbf{R}_{D/A}) \ . \tag{2}$$

Notice the acceleration of the center of vehicle rotation $\mathbf{A}_O$ corresponds to accelerations due to pure translation, and that $\mathbf{A}_A$ appears in the last three equations. Then, if $\mathbf{A}_A$ is subtracted from $\mathbf{A}_B$, $\mathbf{A}_C$, and $\mathbf{A}_D$, only the accelerations due to pure rotation remain:

$$\mathbf{A}_B - \mathbf{A}_A = \dot{\mathbf{W}} \times \mathbf{R}_{B/A} + \mathbf{W} \times (\mathbf{W} \times \mathbf{R}_{B/A}) \ ,$$

$$\mathbf{A}_C - \mathbf{A}_A = \dot{\mathbf{W}} \times \mathbf{R}_{C/A} + \mathbf{W} \times (\mathbf{W} \times \mathbf{R}_{C/A}) \ ,$$

$$\mathbf{A}_D - \mathbf{A}_A = \dot{\mathbf{W}} \times \mathbf{R}_{D/A} + \mathbf{W} \times (\mathbf{W} \times \mathbf{R}_{D/A}) \ . \tag{3}$$

Furthermore, $\mathbf{A}_A$, $\mathbf{A}_B$, $\mathbf{A}_C$, and $\mathbf{A}_D$ are measured by four triaxial linear accelerometers providing the following 12 outputs: A_A^X, A_A^Y, A_A^Z, A_B^X, A_B^Y, A_B^Z, A_C^X, A_C^Y, A_C^Z, A_D^X, A_D^Y, and A_D^Z, where A_D^Z is the acceleration at point D in the Z direction, and likewise for the other outputs. Also, since the position of each accelerometer with respect to each other ($\mathbf{R}_{B/A}$, $\mathbf{R}_{C/A}$, $\mathbf{R}_{D/A}$) is known, all the necessary data are readily available to extract the desired angular motion information. Figure 2 shows that

$$\mathbf{R}_{B/A} = R_{B/A}\,\mathbf{i}\ ,$$

$$\mathbf{R}_{C/A} = R_{C/A}\,\mathbf{j}\ ,$$

$$\mathbf{R}_{D/A} = R_{D/A}\,\mathbf{k}\ , \tag{4}$$

where **i, j,** and **k** are the orthogonal unit vectors for the $X'Y'Z'$ frame. Substituting these values, and expanding the acceleration equations for $\mathbf{A}_B$, $\mathbf{A}_C$, and $\mathbf{A}_D$ in the direction of each axis, the following identities result:

$$A_B^X = [A_A^X - R_{B/A}(W_Y^2 + W_Z^2)]\ ,$$

$$A_B^Y = [A_A^Y + R_{B/A}\ (\dot{W}_Z + W_X W_Y)]\ ,$$

$$A_B^Z = [A_A^Z - R_{B/A}(\dot{W}_Y - W_X W_Z)]\ , \tag{5}$$

$$A_C^X = [A_A^X - R_{C/A}(\dot{W}_Z - W_X W_Y)]\ ,$$

$$A_C^Y = [A_A^Y - R_{C/A}\ (W_X^2 + W_Z^2)]\ ,$$

$$A_C^Z = [A_A^Z + R_{C/A}(\dot{W}_X + W_Y W_Z)]\ , \tag{6}$$

$$A_D^X = [A_A^X + R_{D/A}(\dot{W}_Y + W_X W_Z)]\ ,$$

$$A_D^Y = [A_A^Y - R_{D/A}(\dot{W}_X - W_Y W_Z)]\ ,$$

$$A_D^Z = [A_A^Z - R_{D/A}\ (W_X^2 + W_Y^2)]\ . \tag{7}$$

The systems of Eqs. (5), (6), and (7) can be modified to obtain expressions for the angular accelerations, based on the outputs of the linear accelerometers (A_A^X through A_D^Z) for each of the orthogonal axes of a reference frame. This results in a new system of equations:

$$\dot{W}_X = (A_C^Z - A_A^Z)/(2R_{C/A}) - (A_D^Y - A_A^Y)/(2R_{D/A})\ ,$$

$$\dot{W}_Y = (A_D^X - A_A^X)/(2R_{D/A}) - (A_B^Z - A_A^Z)/(2R_{B/A})\ ,$$

$$\dot{W}_Z = (A_B^Y - A_A^Y)/(2R_{B/A}) - (A_C^X - A_A^X)/(2R_{C/A})\ . \tag{8}$$

The system of Eq. (8) demonstrates that nine linear accelerometers can be used to sense angular accelerations in three axes, seven linear accelerometers for two axes, and four for a single axis.

3 Accelerometer-Based Stabilization System

Conventional servo systems operating the gimbals usually work in a position-control mode where angular orientation is regulated. It is preferable to operate them in a velocity-control mode where angular rate is controlled because the system bandwidth is increased. Using accelerometers allows the servo system to operate in an acceleration-control mode, which is even more desirable because this further increases the stabilization bandwidth. The inertial stabilization of an imaging system is obtained by forcing gimbal rotations countering those of the vehicle, urging the sensed angular accelerations toward zero (accelerometers on-gimbal), or measuring vehicle angular accelerations and commanding calculated counterrotations (accelerometers off-gimbal) so that the image is stabilized.[6]

The accelerometers on-gimbal configuration follows more classical stabilization systems, where the angular motion sensors are placed directly on the stabilized object. The sensor on-gimbal configuration is often referred to as *mass stabilized.*[7] Vehicle motion inputs activate the servo motors in the gimbal system. They generate a motion equal in magnitude, and opposite in direction, that stabilizes the platform by urging the sensed angular acceleration toward a null value. The advantage of this configuration is that the accelerometers act as direct feedback elements in the control loop, forcing the vehicle and gimbal motion to be synchronized (although opposite in direction) at all times.

Figure 3 shows a schematic of a stabilized imaging sensor suite. The unit consists of a three-axis gimbal system carrying a pair of TV cameras for stereo vision. The roll axis (innermost rotation) has freedom to rotate with respect to the pitch axis, which in turn rotates relative to the yaw axis (outermost rotation). Four linear accelerometers are attached to the inner gimbal as shown. One is positioned at the intersection of three orthogonal sensor suite axes and measures three-axis linear accelerations. The other three are located along the orthogonal axes and measure two-axis linear acceleration in each of three orthogonal planes. The TV cameras' angular accelerations in roll, pitch, and yaw are extracted from the linear acceleration measurements by combining the accelerometer outputs as described by the system of Eq. (8). The control system strategy is to force gimbal rotations that counteract the vehicle angular rotations so the net sensed angular accelerations are urged toward a null value. Figure 4 shows a diagram of the control system accomplishing this objective.

Figure 5 shows a block diagram of a single-axis gimbal controller. Stabilization of the TV cameras is accomplished by the bottom feedback loop in Fig. 5 since accelerometers are inertial sensors. In other words, any vehicle-induced angular motion of the TV cameras will be sensed by accelerometers. The stabilization loop will command the servo motor to counteract it so that the combined motion, camera-to-vehicle and vehicle-to-inertial space, is null. On the other hand, the position sensor (i.e., optical encoder, resolver, etc.) is not inertial. It only measures those camera rotations relative

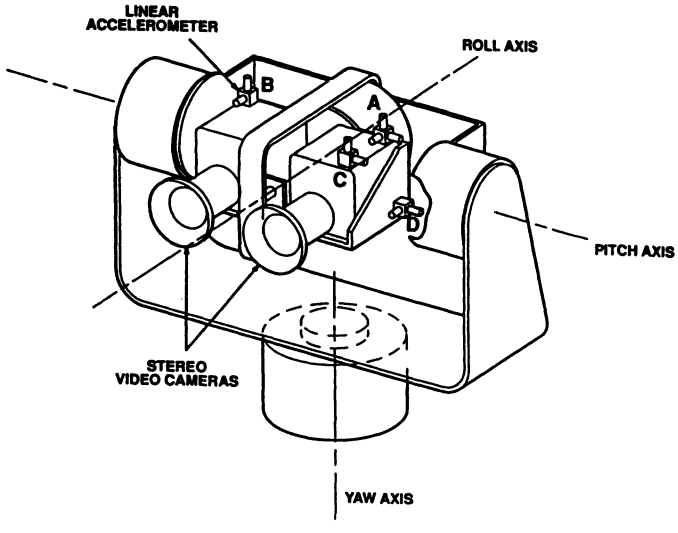

Fig. 3 Stabilized imaging sensor suite.

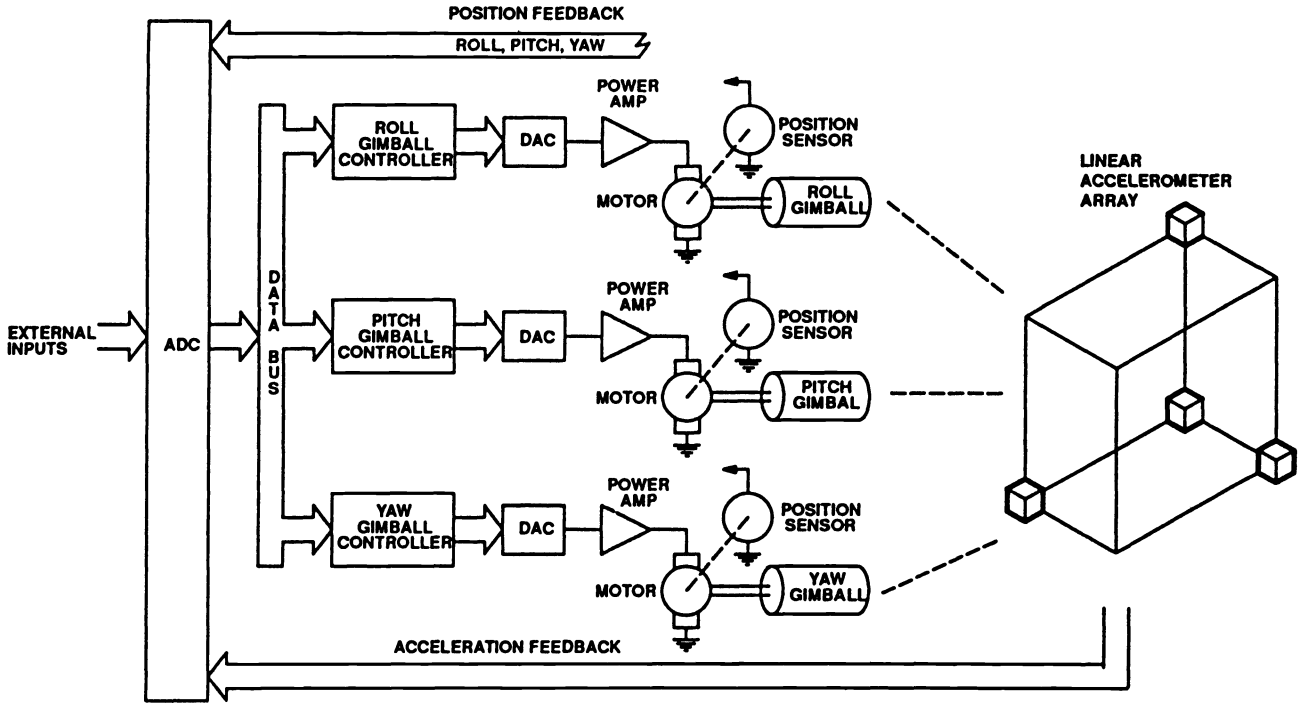

Fig. 4 Control system block diagram.

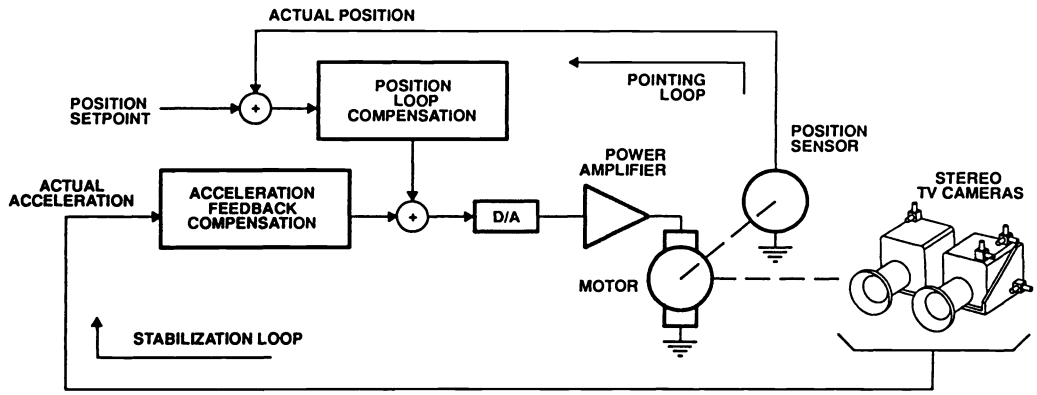

Fig. 5 Single-axis gimbal controller block diagram.

to the vehicle to allow pointing the cameras with respect to the vehicle axes. In an alternative application, the pointing loop could be replaced by a tracking loop maintaining the cameras on target at all times, or by an inertial type sensor (such as an inclinometer) if pointing with respect to a fixed reference frame is desired. At first glance, the stabilization and pointing loops in Fig. 5 appear to be in conflict because any gimbal rotations required to reject vehicle rotations would be fought by the pointing loop controlling the camera orientation relative to the vehicle. However, if the pointing loop has low-pass characteristics, and the stabilization loop has bandpass characteristics, the dual role of stabilization and pointing can be implemented simultaneously.

As an application example,[8] consider the driver/mobility video unit of a tactical unmanned ground vehicle (TUGV). This unit allows the operator to drive the vehicle from a remote location by providing imagery of the road ahead. Figure 3 is also representative of this system. TUGVs are designed for all-terrain and all-weather use. As the vehicle moves over the road and off the road, the chassis is subject to linear oscillations, called surging, lurching, and bouncing, and to angular motion in roll, pitch, and yaw. These disturbances, caused by both vehicle dynamics and road roughness, lead to image motion. The contribution of vehicle inertial dynamics to body angular motion is related to the load transfer while braking, accelerating, and cornering. This causes the body to pitch and roll. Yaw is also observed when cornering beyond a change in heading, and it is due to an imbalanced torque caused by the tire side forces and the steering forces (understeering or oversteering behavior). Even though the total angular displacements could become significant under hard cornering or braking conditions, the motion time constant is relatively large, no less than 1 s. Therefore, they should not be considered as jitter. Angular vibrations caused

by road roughness have higher frequency components and can be properly categorized as jitter.

From Fig. 5, the stabilization loop (with bandpass characteristics) rejects the angular disturbances caused by the vehicle riding over bumps, potholes, rocks, branches, washboard surfaces, and other road irregularities (high frequency, i.e., jitter motion). The pointing loop (with low-pass characteristics) maintains the desired TV camera orientation relative to the vehicle, providing feedback about general terrain characteristics and vehicle dynamics. The stiffness of the pointing loop can be changed by adjusting its gain and bandwidth. This electronically implements different suspension-like effects that can be changed on the fly. The low-pass and bandpass corner frequencies can also be changed at will, based on driver preference and/or terrain characteristics, so that any potential motion-sickness effects can be neutralized. This gives a feel for the road that significantly enhances the driver's ability to safely operate the TUGV, particularly as speed increases and road conditions deteriorate.

4 Proof-of-Concept Unit and Test Results

The development of a proof-of-concept unit was performed under sponsorship by the CAI Division of Recon/Optical, Inc. The objective of the project was to build a basic prototype demonstrating the principle of using linear accelerometers to stabilize about a platform's rotational axis (accelerometers on-gimbal configuration). This effort constituted the first step in bringing accelerometer-based stabilization system (ABSS) technology beyond the conceptual stage. The mechanical design was kept to a minimum and the hardware selection was limited to laboratory supplies and equipment on hand. Figure 6 shows the proof-of-concept system with two linear accelerometers mounted on the gimbal inner structure, approximately 6 in. apart on a horizontal plane. These measure accelerations in the vertical direction (only one accelerometer is shown). Bearing assemblies are provided at both ends, and a dc motor and potentiometer (serving as the position sensor) are located on the left side. This complete assembly mounts onto the base plate of a motion simulator as shown in Fig. 7. Also shown are two power supplies, a signal conditioning board, and a personal computer with an analog-to-digital and digital-to-analog conversion card used to implement the digital control system.

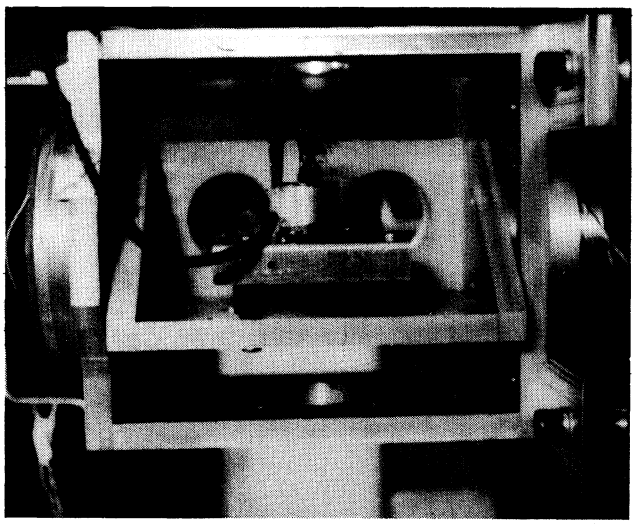

Fig. 6 Proof-of-concept unit.

The stabilization test consisted of disturbing the base with a rotation of approximately ± 5 deg. The base motion had a fundamental frequency of 4 Hz and numerous harmonics. A power spectrum of this motion is shown in Fig. 8. The power at the fundamental frequency was 2.1 dB corresponding to an rms angular acceleration of 1.3 rad/s^2. The angular motion power spectrum for the platform stabilized element is shown in Fig. 9. The power at the fundamental frequency was -26.6 dB corresponding to a 0.0468 rad/s^2 rms value. The ratio between the values for residual platform motion shows that 3.6% of the disturbance was transmitted. This value is not exceptional when compared to transmissibility values of about 1% typical of active stabilization systems. However, the ABSS performance is expected to significantly improve when the important issues of bearing friction, gimbal unbalance, motor current regulator errors, etc. are considered in the design of a refined prototype unit.

5 Summary and Conclusions

This paper presents a new platform stabilization approach where gyroscopes are replaced by linear accelerometers to

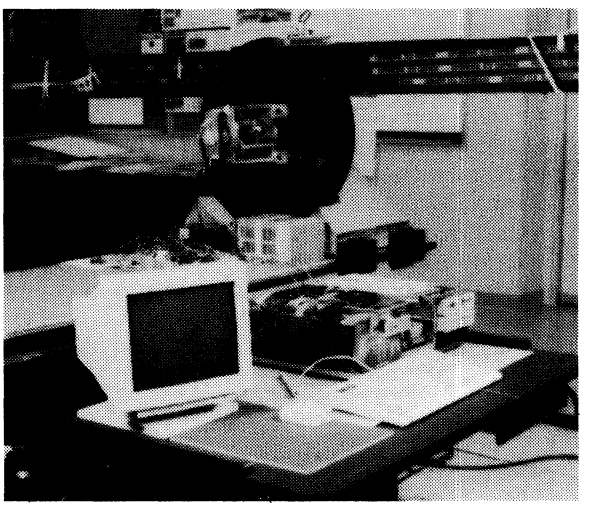

Fig. 7 Proof-of-concept test setup.

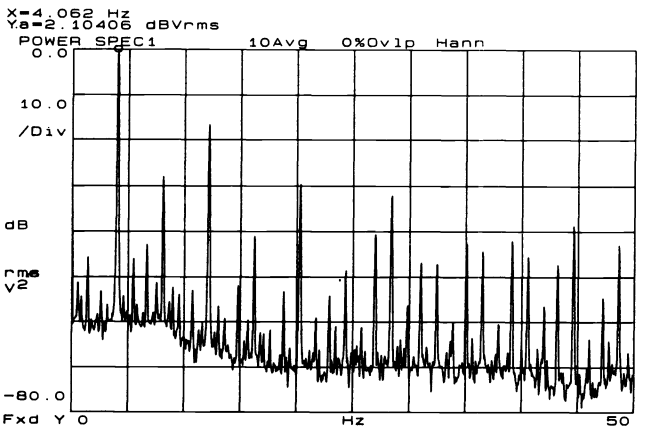

Fig. 8 Base motion power spectrum.

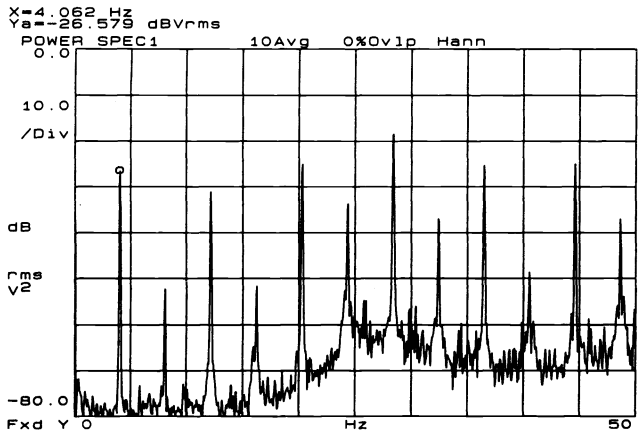

Fig. 9 Stabilized platform residual motion power spectrum.

reduce cost. This substitution provides the additional benefits of less weight and power consumption, better temperature characteristics, more robustness, and higher shock resistance. The means for sensing angular accelerations with linear accelerometers are discussed, and block diagrams of the control system implementing the stabilization strategy are provided, demonstrating the simplicity of the ABSS. The driver/mobility video unit of a TUGV is discussed as an ABSS application to stabilize the image of the road that is displayed to the remote driver. For this example, we show how to electronically implement a suspension-like effect to reject undesirable angular disturbances caused by the vehicle going over potholes, rocks, and other road irregularities, while retaining the motion related to vehicle dynamics and general terrain characteristics. This unique feature of the ABSS provides a feel for the road that significantly enhances the remote driver's ability to operate the vehicle safely. A basic, single-axis, proof-of-concept prototype has been built, and experimental stabilization tests were conducted with very encouraging results.

References

1. A. F. D'Souza and V. K. Garg, *Advanced Dynamics, Modeling and Analysis,* Prentice-Hall, New York (1984).
2. A. J. Padgaonkar, K. W. Krieger, and A. I. King, "Measurement of angular acceleration of a rigid body using linear accelerometers," *Transactions of the ASME,* pp. 552–556 (Sep. 1975).
3. A. Schuler, A. Grammatikos, and K. Fegley, "Measuring rotational motion with linear accelerometers," *IEEE, Annual East Coast Conference on Aerospace and Navigational Electronics,* Baltimore, Maryland, pp. 1–10 (Oct. 1965).
4. A. S. Hu, "Angular acceleration measurement errors induced by linear accelerometer cross-axis coupling," *The Shock and Vibration Bulletin,* Number 50, Part 2, pp. 11–16 (Sep. 1980).
5. D. Galler and A. Booth, "The shocking truth of accelerometer selection," *Machine Design,* pp. 85–89 (July 6, 1989).
6. M. C. Algrain, "Gyroless platform stabilization techniques," U.S. Patent No. 5,124,938 (1992).
7. M. K. Masten and L. A. Stockum, "Electro-Optical-Mechanical Design for Precision Stabilization and Tracking Systems," SPIE Short Course Notes (1990).
8. M. C. Algrain, "A novel, low-cost stabilized driver module for TUGV applications," *3rd Mini Symposium of the Assoc. of Unmanned Vehicle Systems,* Warren, Michigan (Nov. 1990).

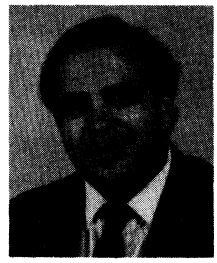

Marcelo C. Algrain received a BSME in 1980 and an MSEE in 1981, both from Wright State University, and a PhD in electrical engineering from the Illinois Institute of Technology in 1991. Since 1991 he has been an assistant professor at the University of Nebraska-Lincoln. From 1989 to 1991, he held the position of engineering specialist at Recon/Optical, Inc., where he performed analyses on stabilization and control systems for high-resolution reconnaissance systems. From 1984 to 1989, he was with Borg-Warner Research developing control system prototypes for a variety of automotive and industrial products. Prior to Borg-Warner, he was with Babcock & Wilcox designing process control systems for nuclear power plants. Dr. Algrain is a member of the SPIE, IEEE, and the AIAA. He has published numerous papers in the control systems field and holds two patents. His research interests are in stabilization, pointing and tracking systems, and stochastic, optimal, and adaptive controls.